

# The protective effect of osmoprotectant TMAO on bacterial mechanosensitive channels of small conductance MscS/MscK under high hydrostatic pressure

Evgeny Petrov,<sup>1,\*</sup> Paul R. Rohde,<sup>1</sup> Bruce Cornell<sup>2</sup> and Boris Martinac<sup>1</sup>

<sup>1</sup>Victor Chang Cardiac Research Institute; Darlinghurst, NSW Australia; <sup>2</sup>Surgical Diagnostics PL; St. Leonards, NSW Australia

**Keywords:** MscS, MscK, TMAO, patch-clamp, bacteria

**Abbreviations:** HHP, high hydrostatic pressure; MscS, mechanosensitive channel of small conductance; MscK, K<sup>+</sup>-dependent mechanosensitive channel of small conductance; TMAO, trimethylamine N-oxide; TM, transmembrane; MS, mechanosensitive; MscL, mechanosensitive channel of large conductance

Activity of the bacterial mechanosensitive channels of small conductance MscS/MscK of *E. coli* was investigated under high hydrostatic pressure (HHP) using the “flying-patch” patch-clamp technique. The channels were gated by negative pipette voltage and their open probability was measured at HHP of 0.1 to 80 MPa. The channel open probability decreased with increasing HHP. When the osmolyte methylamine N-oxide (TMAO) was applied to the cytoplasmic side of the inside-out excised membrane patches of *E. coli* giant spheroplasts the inhibitory effect of HHP on the channel activity was suppressed at pressures of up to 40 MPa. At 40 MPa and above the channel open probability decreased in a similar fashion with or without TMAO. Our study suggests that TMAO helps to counteract the effect of HHP up to 40 MPa on the MscS/MscK open state by “shielding” the cytoplasmic domain of the channels.

## Introduction

Throughout the course of evolution, deep-sea organisms developed a set of mechanisms protecting them from the effects of HHP, a major determinant of their habitat. Physically, HHP is scalar quantity acting in all directions on these organisms at macroscopic as well as microscopic structural levels. Since *in vitro* studies have shown that pressure in the order of one tenth of a MPa can impair quaternary structure of proteins and modify biophysical properties of cell membranes<sup>1</sup> it is of particular interest to understand the mechanisms that provide protection from the effects of HHP at a molecular level.

In an attempt to explain the mechanisms of barotolerance, it has been reported that in tissues of deep-sea fish the concentration of trimethylamine N-oxide (TMAO) strongly correlates with depth at which these organisms live.<sup>2,3</sup> Hence, it appears that TMAO and similar organic osmolytes are key compounds providing barotolerance for deep-sea organisms. Although there is no similar report on protective effect of TMAO in deep-sea bacteria, it has been reported that deep-sea bacteria accumulate the osmolyte  $\beta$ -hydroxybutyrate when exposed to high hydrostatic pressure as well as to osmotic pressure.<sup>2,4</sup> It has also been shown that high intracellular levels of sucrose and lactose

provided protection against cell death induced by high pressure in *Lactococcus lactis*.<sup>5</sup>

Presumably, TMAO provides primarily protection for cytoplasmic proteins. TMAO does not react with protein backbones directly, but coordinates water around them.<sup>6</sup> Although there is no universal molecular theory, which would explain how osmolytes interact with proteins to affect the stability of their structure, according to a recently proposed model by Street et al. (2006),<sup>7</sup> protecting osmolytes such as TMAO push the structural equilibrium in the protein folding reaction toward folded protein structure by being excluded from direct interaction with the protein surface. Under HHP the “TMAO shield” thus prevents penetration of water into protein molecules and preserves their tertiary and quaternary structure. This is an attractive hypothesis accounting well for protection of soluble cytoplasmic proteins under HHP. In the case of membrane-bound or integral membrane proteins their functionality depends on lipid environment of the membrane bilayer, whose structural organization also changes under HHP.<sup>8</sup> HHP in the range of 0.1–50 MPa does not denature the majority of proteins, however, it can affect their structure and function by inducing minor changes in tertiary and quaternary structure or, in the case of integral membrane proteins, by affecting the structure of the lipid environment.<sup>9–11</sup>

\*Correspondence to: Evgeny Petrov; Email: petrov67@gmail.com  
Submitted: 05/07/12; Revised: 06/14/12; Accepted: 06/20/12  
<http://dx.doi.org/10.4161/chan.20833>

The aim of this study was to discern between the effects that HHP exerts on the lipid bilayer and a membrane protein by examining the effect of HHP on the activity of the mechanosensitive (MS) channels of small conductance of *E. coli* using the “flying-patch” patch-clamp method (see Figure 2 in Macdonald and Martinac 2005), in the presence or in the absence of TMAO. In this study we also provide evidence that both MscS and MscK are responsible for observed effect of HHP on the channel open probability. Specifically, we investigated whether HHP would exert its effect on the MscS/MscK channels via the membrane bilayer, directly on the channel protein or on both. As one of the three types of MS channels found in bacteria,<sup>12,13</sup> MscS has been extensively studied in giant spheroplasts of *E. coli*<sup>14,15</sup> as well as by reconstitution of *E. coli* membrane fractions or purified channel proteins into liposomes.<sup>15–18</sup> Membrane tension produced by stretching the lipid bilayer alone is the primary stimulus required for activation and gating of this MS channel.<sup>19,20</sup> The channel activity is also modulated by voltage, such that membrane depolarization favors the channel opening.<sup>14,21</sup> The 3D crystal structure of MscS reveals that the channel is a homoheptamer<sup>22,23</sup> in which each subunit is composed of three transmembrane (TM) segments, TM1, TM2 and TM3 as well as a large cytoplasmic region. The TM3 helices line the channel pore whereas the TM1 and TM2 helices have been proposed to constitute the sensors for membrane tension and voltage.<sup>22,24</sup> At present there is no crystal structure for MscK available. However, the alignment of primary amino acid sequences of MscS vs. MscK reveals 45% similarity for the region that the much longer MscK overlaps with the full length of MscS.<sup>25</sup>

There are several reasons for choosing MscS/MscK in our study of the HHP effects on MS channels: (1) the activity of MscS/MscK is tightly controlled by the physical forces in the lipid bilayer,<sup>19,26</sup> (2) during its gating between the closed and open states MscS undergoes large conformational changes,<sup>21,27</sup> (3) the cytoplasmic C-terminal domain of MscS/MscK presents a large portion of the channel protein outside of the membrane bilayer, and (4) the activity of MscS under HHP has been partially investigated in previous studies.<sup>28,29</sup> Using MscS/MscK for HHP experiments in this study has also the advantage of being able to gate the channel by voltage.<sup>14</sup> This is advantageous since controlling the negative pressure applied to a patch pipette (required for stretching a spheroplast patch) in the high pressure chamber is currently not technically possible at the current stage.

The role of the MscS cytoplasmic domain in gating of the channel is not well understood. The current view is that the chamber is a dynamic structure that undergoes significant conformational changes upon the channel gating.<sup>30</sup> During gating the cytoplasmic domain passively follows the movement of the “hairpin” formed by the transmembrane TM1 and TM2 helices<sup>22,29,31</sup> as well as following the expansion of the aqueous pore, lined with TM3 helices. The cytoplasmic domain is also considered to play a role in voltage-independent adaptation of the channel.<sup>30,32</sup> It has also recently been suggested that this domain may serve as a sensor of cytoplasmic crowding.<sup>33</sup> The MscK structure-and-function details are not clarified well yet, but its biophysical properties, such as mechanosensitivity, conductance

and gating and amino acid sequence alignment to MscS suggests that its membrane part and cytoplasmic domain are similar to MscS.<sup>34</sup> Given their similarities and taking into consideration that MscS and MscK ion currents are difficult to distinguish electrophysiologically from each other,<sup>35</sup> we treated the channels in this study together as one channel—MscS/MscK. Overall, our study suggests that TMAO could stabilize the C-terminal cytoplasmic portion of MscS/MscK by coordinating water around it<sup>6,7</sup> and this could stabilize the channel structure and gating under HHP.

## Results

**Voltage dependence of MscS.** Given that in our present study activation of MscS/MscK by voltage was essential to conduct the experiments under HHP, we examined the voltage dependence of MscS upon reconstitution into tethered bilayers (Materials and Methods). The choice of a tethered bilayer for these experiments has the advantage that the bilayer is not mechanically stressed, so that examining the voltage dependence under these conditions should be free from potential interference with activating the channels by membrane tension in addition to voltage. As shown in Figure 1, MscS channels behaved in a voltage-dependent manner by showing more activity at positive membrane potentials compared with negative potentials. In contrast, MscL, which was used as a control, did not exhibit any voltage dependence. MscS responded in a voltage-dependent manner in tethered membranes, whereas the MscL showed only a small effect at a very high voltage, which was likely associated with leakage conduction through the supporting lipid. As previously established the activity of MscL depends purely on membrane tension<sup>40,41</sup> In addition, comparison with protein free lipid was used as another control that indicated the voltage dependency was a property of MscS and not the tethered membrane. These control experiments gave us additional confidence to examine MscS/MscK behavior under HHP.

**Inhibitory effect of HHP on the MscS/MscK activity.** MscS/MscK was activated by applying negative voltage to the patch pipette corresponding to a depolarizing membrane potential in the inside-out spheroplast patch recording mode used for the experiments in this study. In the majority of patches the channels began to open at pipette voltages at or more negative than -30 mV. Patches in which channels could be gated by voltages larger than -80 mV were not used for the HHP experiments, because at these voltages patches tended to break during HHP application at pressures higher than 40 MPa. If channels exhibited steady-state activity for 3–4 min after the onset of a recording, this interval was used throughout the study as a control measurement of the MscS/MscK activity at atmospheric pressure of 0.1 MPa. At voltages less negative than -80 mV such steady-state activity was a sufficient indicator to proceed further with recordings during which HHP was increased up to 80 MPa in a step-like fashion. During each pressure step several negative pipette voltages were usually applied to monitor the effect of voltage on the MscS/MscK at a given HHP (Fig. 2A). Generally, upon increasing HHP at a given voltage, the open probability (NPo) of the channels decreased.

At pressures  $\geq 70$  MPa the channels remained closed in most patches examined (Fig. 2C). Closer inspection of recorded traces revealed that, as previously reported, the channels had a tendency to frequently gate at subconducting levels as HHP increased<sup>28</sup> (Fig. 2B, amplitude histograms). Conductance of MscS/MscK was not affected by HHP at all applied pressures (0.1–80 MPa) (Fig. 2B). However, the full open state of the channel was more frequently detectable in the lower range of HHP ( $\leq 40$  MPa) and less frequently in the high range of applied HHP ( $> 40$  MPa) as previously reported (Fig. 3A,<sup>28</sup>). After pressure was released back to atmospheric pressure, in about 65% of the patches examined under HHP ( $n = 8$ ) MscS/MscK fully recovered its voltage sensitivity and fully open state with conductance recorded before the application of HHP<sup>28</sup> (Fig. 2C). In the remaining 35% of the patches the channel activity failed to recover its voltage sensitivity.

**Protective effect of TMAO against HHP.** Based on measurements of TMAO concentration in fresh and sea water species, 100 mM of TMAO is more than sufficient to provide protection against HHP.<sup>2,3</sup> Accordingly, most experiments in this study were performed using 100 mM TMAO. In addition, in four further experiments we used 50 mM TMAO (data not shown). Although we also attempted to examine the effect of HHP at a TMAO concentration of 200 mM, these experiments failed because at this concentration we were not able to obtain sufficiently stable gigaohm seals required for the HHP experiments.

Under atmospheric pressure (0.1 MPa) TMAO at 100 mM in the bath solution had no detectable effect on MscS/MscK conductance (Figs. 2B and 3B) and its voltage-sensitivity (Fig. 3A). Analysis of recordings from 30 patches examined at 100 mM TMAO showed that upon increasing HHP to  $\sim 40$  MPa voltage-dependent activity of the channel was comparable to the channel behavior at atmospheric pressure (Fig. 3A). In contrast, at HHP values  $> 40$  MPa the activity of the channels decreased with increasing pressure similar to the channel behavior recorded under HHP in the absence of TMAO (Fig. 4). This result suggested that TMAO could partially protect the channel structure and gating from the effects of HHP. At concentration of 50 mM TMAO protected the channels against HHP in a similar fashion as at the concentration of 100 mM. MscS/MscK retained its normal voltage-dependent activity at HHP up to  $\sim 60$  MPa (see Fig. 3A).

**Reaction volumes in absence and in presence of TMAO.** According to Le Châtelier's principle, an increase of pressure shifts the equilibrium of a reaction to the state which occupies a lesser volume. Equilibrium systems with two energetically stable states, such as MS channels that exist in two basic conformational states, closed (C) and open (O), can be described in terms of the equilibrium constant  $K$  (given by the open probability  $N_{Po}$ ) of a simple two-state reaction  $C \rightarrow O$ . Decrease in the MscS/MscK open probability  $N_{Po}$  results from an equilibrium shift toward the closed state of the channel, which occupies lesser volume than the open state of the channel.<sup>32,42</sup> Consequently, increasing HHP causes a decrease in the  $N_{Po}$  of MscS/MscK. This is in agreement with the notion that MscS and MscK, like MscL, are MS channels undergoing large

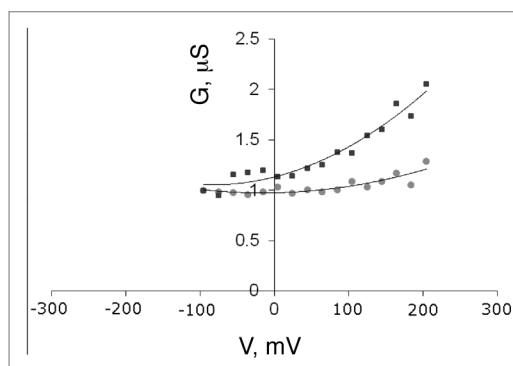


**Figure 1.** Normalized current-voltage relationship for MscS and MscL reconstituted into tethered bilayers. MscS (filled squares) channels exhibit a voltage-dependent behavior by showing more activity at positive as compared with negative membrane potentials. MscL (filled circles) does not exhibit any voltage dependence except at high voltages ( $\sim +200$  mV) possibly due to leakage conduction through the supporting lipid bilayer. These results were obtained from tethered membranes purchased from SDx Tethered Membranes™ and read by an SDx Tethered Membranes TetherPatch™ Potentiostat. In the inner leaflet of the tethered membrane 10% of the lipids were tethered and in the outer leaflet all lipids were mobile. The tethered spacer groups at the surface of the gold electrode were  $\sim 2$  nm in length and the reservoir space between the gold and the inner surface of the membrane were  $\sim 4$  nm in length. It is proposed that these packing densities accommodate both the membrane incorporated and the extra membranous segments of either MscS or MscL while still permitting the conformational and diffusional movements required for a conducting channel. In both cases some spontaneous conduction was evident in the C20 phytanyl (equivalent to a C16 long methylene chain) lipid bilayer used here.

conformational changes during gating between the closed and open states of the channel (i.e. " $t \cdot \Delta A$ ,"  $t$  – membrane tension,  $\Delta A$  – difference in area occupied by open vs. closed channel).<sup>13,32,43-49</sup> The relationship between the equilibrium constant  $K$ , volume change across the equilibrium (i.e., reaction volume)  $\Delta V$  (Moles) and pressure (Pascals) at constant temperature is given by the classical thermodynamic equation:  $[\ln K / dp]_T = -dV / RT$ , where  $T$  is the absolute temperature and  $R$  is the gas constant. In a multi-component system consisting of an ion channel, lipid bilayer, and ionic solution, one would expect that volume changes  $\Delta V$  obtained from linear fits shown in Figure 4 mostly result from the volume changes in the MscS/MscK channel and/or the lipid bilayer given that the bulk water is least compressible among the components of the system.

Calculated from the linear fit of data shown in Figure 4A the compression of spheroplast patches over the range of 0.1 to 80 MPa resulted in a volume change  $\Delta V$  of  $-69$  ml/Mol, corresponding to  $-114 \text{ \AA}^3$  per one channel molecule. This is comparable to the previously published volume change of  $\sim 155 \text{ \AA}^3$ .<sup>28</sup> In comparison, the volume of the channel heptamer of approximately  $6.0 \times 10^5 \text{ \AA}^3$ <sup>28</sup> is quite large compared with the calculated  $\Delta V$ . Possible factors that could contribute to the volume changes caused by the HHP are discussed later together with results obtained in HHP experiments in the presence of TMAO.

In the presence of TMAO, increasing HHP had a differential effect on the MscS/MscK open probability than in the absence of

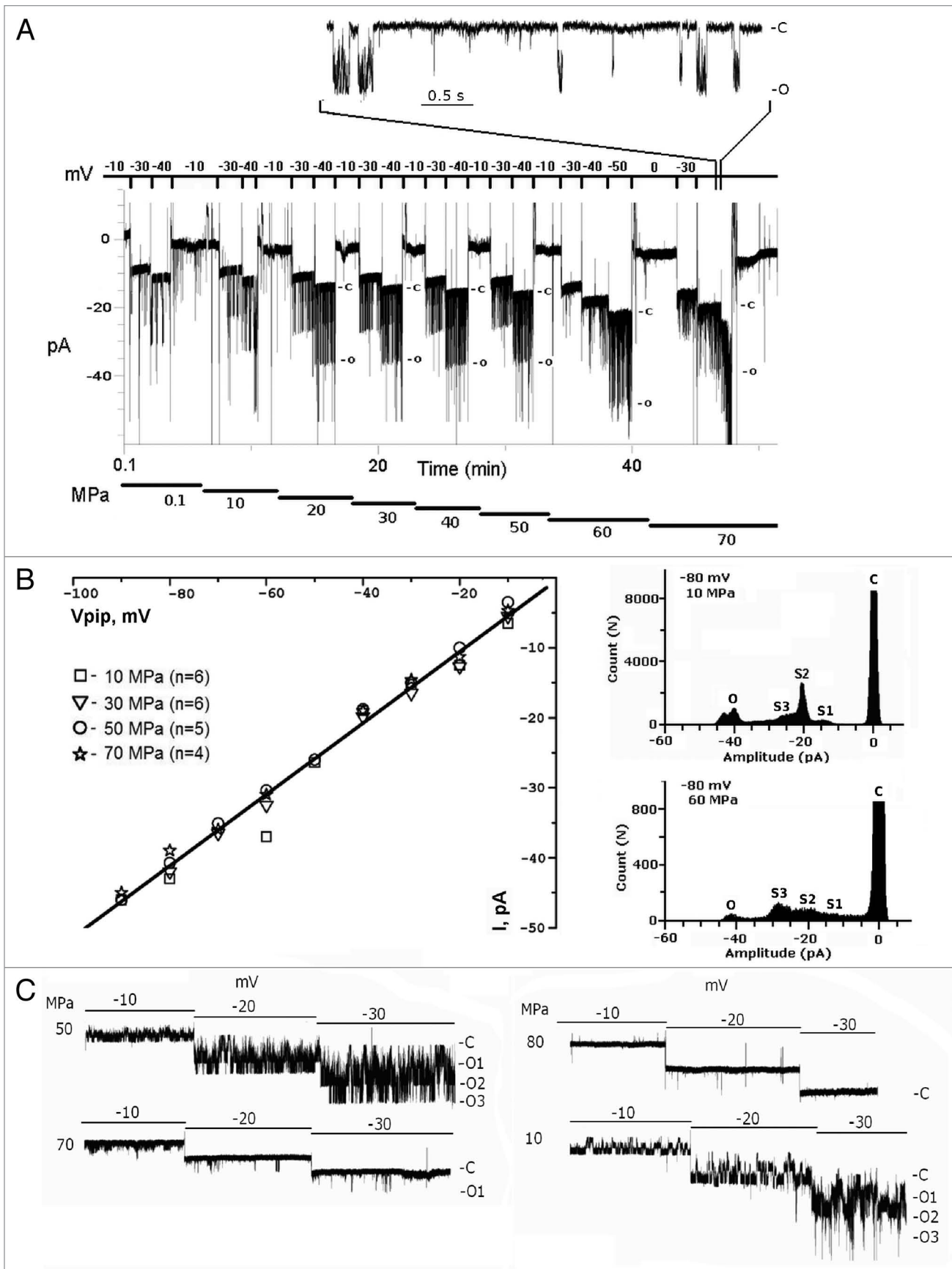


**Figure 2.** For figure legend, see page 266.



**Figure 2 (See previous page).** Effect of HHP and voltage on MscS/MscK open probability and conductance. **(A)** Representative current recordings of MscS/MscK at different pipette voltage and HHP. During each HHP step (see protocol below the recordings) a set of voltages was applied (values are shown above the recordings). Note that upon HHP increase duration of the open states decreased. At HHP > 60 MPa the full open state of MscS/MscK was detected less frequently (see insert showing a current trace on an expanded time scale at 70 MPa). **(B)** Current-voltage relation obtained at different HHP values. Full open states of MscS were detected at all HHP values in the interval 10–70 MPa. MscS/MscK slope conductance of  $0.61 \pm 0.03$  nS obtained at different HHP from 21 patches is the same as at 0.1 MPa. The number of patches *n* examined at particular HHP is given in parentheses at each symbol. Amplitude histograms obtained at HHP of 10 and 60 MPa and at -80 mV pipette voltage demonstrate that MscS/MscK opens fully at different levels of HHP (C, closed state; O, open state; S<sub>n</sub>, subconducting states of the channel) **(C)** Representative recording of MscS/MscK under different steps of HHP and voltages. Note the recovery of channels gating when pressure was released back to 10 MPa

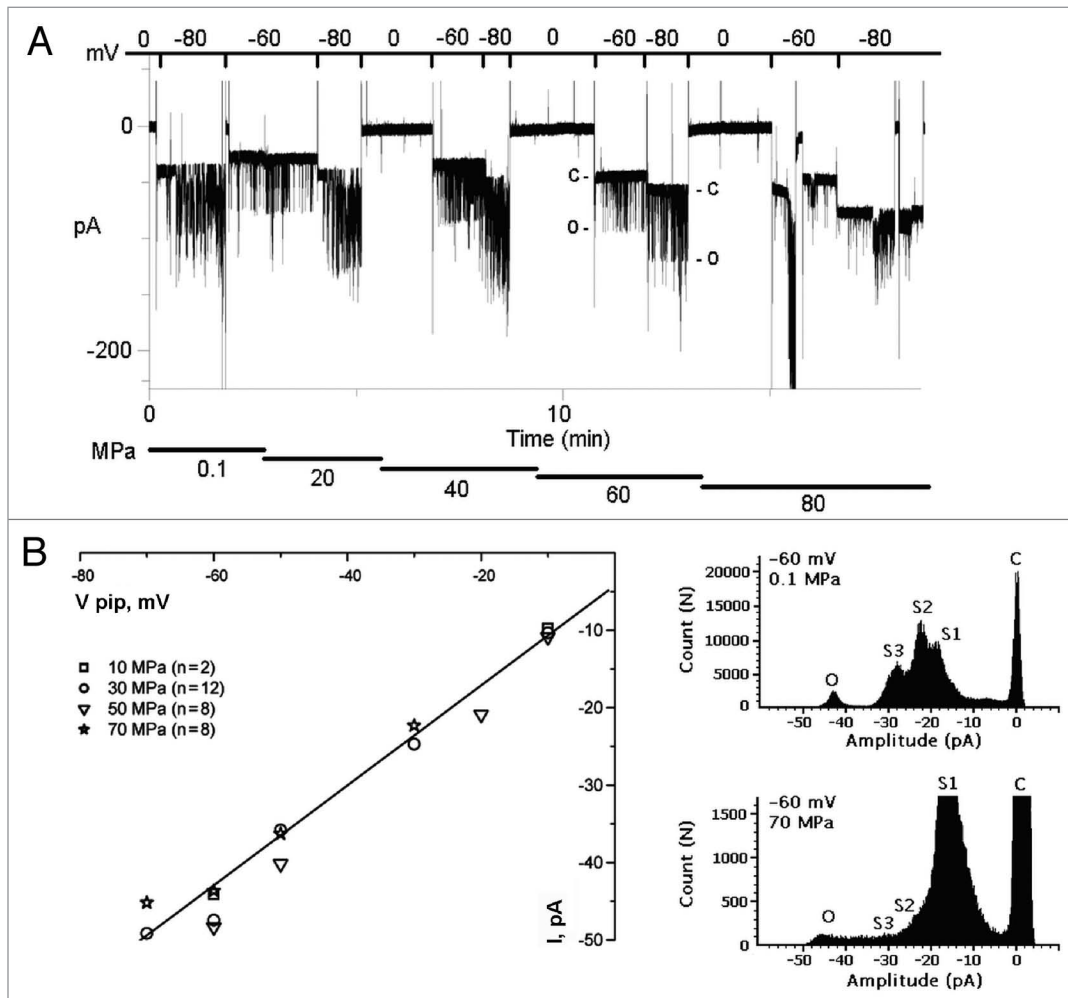


**Figure 3.** Effect of HHP and voltage on MscS/MscK open probability in presence of TMAO. **(A)** Current recordings of MscS/MscK at different pipette voltages and HHP in the presence of 100 mM TMAO. **(B)** Current-voltage relation obtained at different HHP in the presence of 100 mM TMAO. MscS/MscK slope conductance of  $0.64 \pm 0.02$  nS obtained at different HHP from 30 patches is the same as one obtained in the absence of TMAO indicating that TMAO did not affect conductance of the channel. Amplitude histograms were obtained at HHP of 0.1 and 70 MPa at -60 mV. C, O and S<sub>n</sub> denote closed, open and subconducting levels of the channel, respectively. **(C)** 3D graph showing MscS/MscK open probability  $NP_o$  similar as in Figure 2C but in the presence of 100 mM of TMAO. Note that  $NP_o$  remained very similar in the interval 0.1–50 MPa.

TMAO. Over the range of HHP between 0.1 to 40 MPa linear fit of data shown in Figure 4B gave a volume change of  $\Delta V = -8.1$  ml/Mol. This corresponds to approx.  $-13 \text{ \AA}^3$  per one MscS/MscK molecule. The approximate linear fit of data over the interval 40 to 80 MPa gave a reaction volume  $\Delta V = -130$  ml/Mol corresponding to  $-216 \text{ \AA}^3$  per MscS/MscK channel molecule. It is higher than the free volume change calculated in the absence

of TMAO, which means that above 40 MPa, MscS/MscK was more susceptible to HHP despite the presence of 100 mM of TMAO. It is possible that at pressures > 80 MPa phase transition of phospholipid membrane might occur in some cases,<sup>50</sup> which could irreversibly affect the lipid-MscS/MscK interactions thus preventing the restoration of the channel function upon release of HHP.

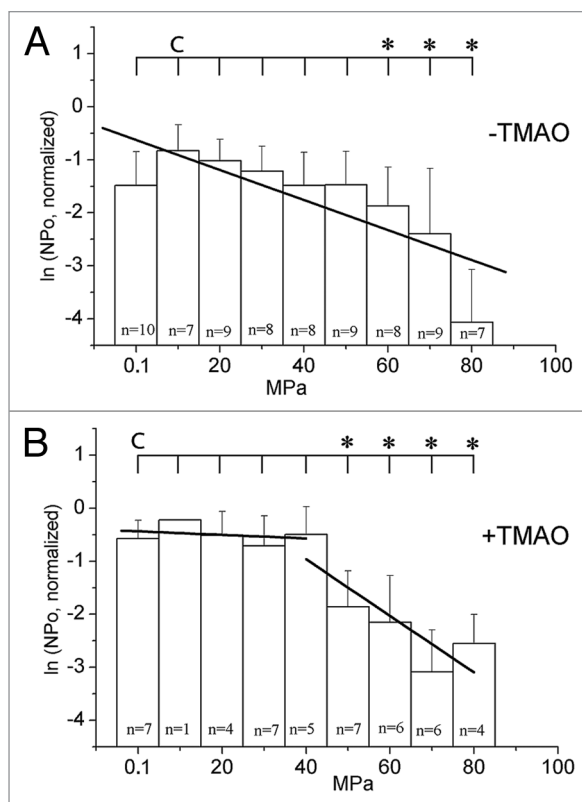


**Figure 4.** Effect of TMAO on volume changes under HHP. Semilogarithmic plot of normalized NPo values (averaged from NPo values obtained from recordings at all voltages at a particular HHP) vs. hydrostatic pressure shows a linear relationship. The number n in each histogram indicates the number of measurements obtained at different voltages at each pressure step. **(A)** The experimental points obtained in the absence of TMAO were fitted over the whole range of HHP applied during the experiments (0.1–80 MPa). Each vertical bar is represented as  $\ln(\text{mean})$  and error given by  $\pm [\ln(\text{mean} + \text{S.E.}) - \ln(\text{mean})]$  of n measurements. Single linear fit gave a volume change across the equilibrium  $\Delta V$  of  $-69 \text{ ml/mol}$  (i.e.,  $-114 \text{ \AA}^3$  per channel molecule) (see Results). **(B)** The experimental points obtained in the presence of 100 mM TMAO were fitted by two linear fits, the first one in the 0.1–40 MPa range and the second one in the 40–80 MPa pressure range giving volume changes of  $-8.1 \text{ ml/Mol}$  (i.e.,  $-13 \text{ \AA}^3$  per channel molecule) and  $-130 \text{ ml/Mol}$  (i.e.,  $-216 \text{ \AA}^3$  per channel molecule), respectively (see Results). Linear fit to histograms is made for the purpose of approximate estimation of free volume change of MscS/MscK under HHP. The pair-wise comparison using Student t-test of the vertical bars in both histograms in this figure showed the statistical difference at  $p < 0.05$  significance level between the control bar (marked with C on the horizontal line above each histogram) and vertical bars corresponding to HHP values marked by asterisks.

## Discussion

The MscS/MscK modulation by voltage allows these channels to be examined in a high-pressure chamber in which it cannot be activated by membrane tension. Despite current evidence suggesting that MscS activity could only be modulated by voltage once the channel is activated by membrane tension<sup>51,52</sup> we were able to establish that MS channel could be activated by voltage in tethered bilayers independently of membrane tension (Fig. 1).

Generally, HHP affected the channel kinetics such that the open probability decreased with increasing pressure. As previously reported,<sup>28</sup> the MscS also exhibited frequent gating at subconducting levels with increase in HHP although its main conductance corresponding to the fully open state of the channel remained overall unaffected by HHP. Volume compressibility of phospholipid membrane is less than 1% at 100 MPa<sup>53</sup> and compressibility of the bilayer in the horizontal plane is higher than in the vertical plane.<sup>8</sup> Furthermore, it has been reported that pressurization of the oriented 1,2-dimyristoyl-sn-glycero-3-phosphatidylcholine/cholesterol bilayers results in an in-plane compression of 3–7% at 190 MPa corresponding to increase in the thickness of the bilayer by approximately  $1.5 \text{ \AA}$ .<sup>54</sup> This roughly corresponds to an increase of  $0.6 \text{ \AA}$  in the bilayer thickness at 80 MPa in our experiments. Since changes in the physical properties of the lipid bilayer affect functioning of MS channels<sup>28,44,55,56</sup> it is possible that the effects of HHP on MscS/MscK are also due to the effects on the lipid bilayer, as previously discussed.<sup>28</sup> MscS activity is dependent on mobility of the TM1-TM2 “hairpin” and thus it is dependent on how tightly boundary phospholipids are packed. Given its sequence similarity to MscS this may also be applicable to MscK as well. Consequently, the increased packing of phospholipid hydrocarbon chains under HHP<sup>10</sup> would be expected to limit the TM1-TM2 mobility within the bilayer. In a more viscous membrane the channels would tend to remain closed due to immobilization of the TM1-TM2 transmembrane domains in densely packed hydrocarbon chains making it more difficult for the TM helices to move when voltage is applied (Fig. 5A).

In the current study, 50 and 100 mM TMAO protected the MscS/MscK channel from the effects of HHP, such that MscS at HHP within the 0.1–40 MPa range gated to similar extent at all pressures within this range (Figs. 3A, 5B1 and 5B2). However, upon further increase in HHP, NPo decreased as if TMAO was not present (Fig. 5.3). This suggests that the protective effect of TMAO was abolished in a threshold-like manner within the 40–80 MPa pressure range. This result seems to indicate that HHP may not only be affecting the lipid bilayer but also the MscS/MscK protein itself. Since TMAO is a small molecule it could diffuse easily through water-accessible parts of MscS/MscK without interacting with the protein surface by forming a “protective shield” around the folded structure of the protein,<sup>7</sup> such that the channel protein structure is protected from HHP (Fig. 5).

According to a generally accepted model of MscS gating,<sup>42,52</sup> TM1-TM2 “hairpin” of each subunit is moving across the membrane bilayer during gating causing a straightening of the TM3 helices to remove a kink midway through the membrane, establishing contact between TM3 and TM2 helices and thus enabling opening of the MscS pore.<sup>51</sup> Furthermore, the large cytoplasmic domain extends a long way from the membrane and contains a large central chamber accessible through seven side openings and one distal pore.<sup>23,57</sup> The conformation of the cytoplasmic domain has also been shown to influence the conductivity of the pore,<sup>51</sup> such that it passively follows TM1-TM2-TM3 complexes and expands as a “Chinese lantern.”<sup>58</sup> In the presence

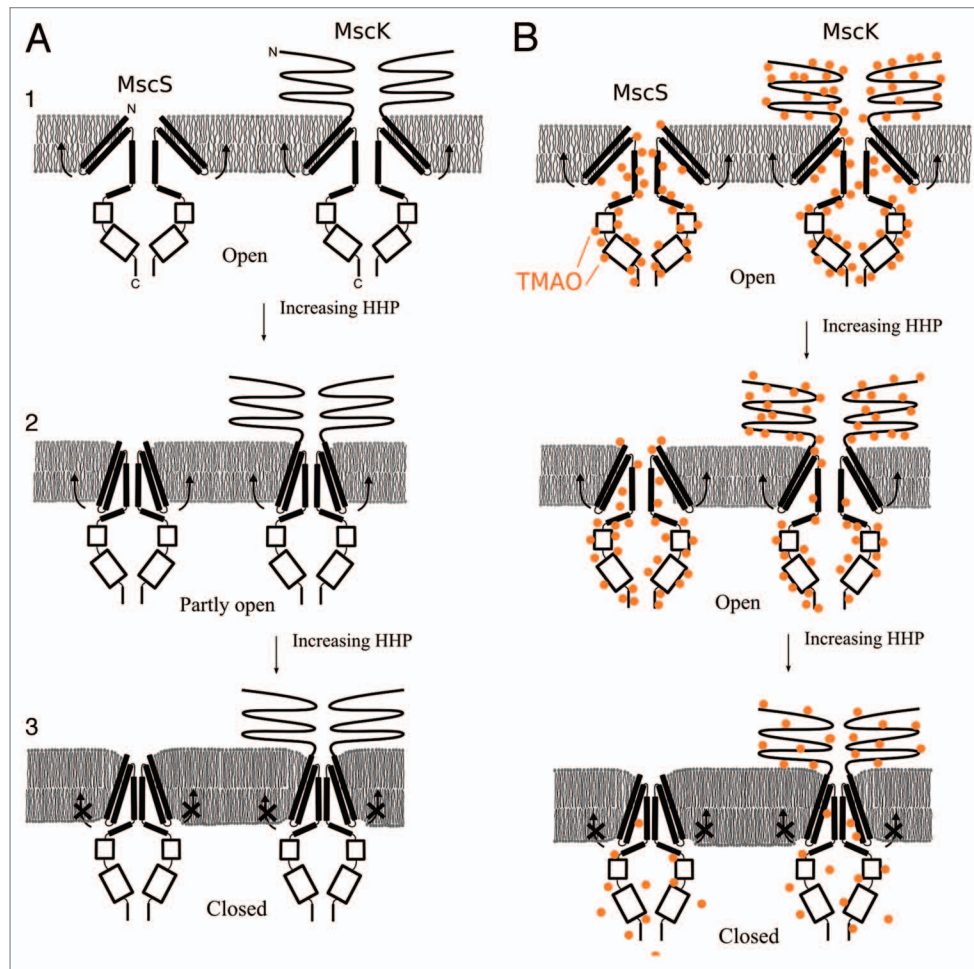


**Figure 5.** Model of MscS and MscK gating by voltage under hydrostatic pressure in the absence (A) and presence of TMAO (B). (1) Voltage-dependent MscS and MscK closed-open transitions. Depolarizing membrane voltages (corresponding to negative pipette voltages more negative than  $-40$  mV in inside-out excised spheroplasts patches) force TM1-TM2 helices (TM1-TM2 “hairpin”<sup>29,31</sup>), harboring positively charged arginins, to move apart and up toward the opposite side of the bilayer.<sup>22,59</sup> Arrows indicate direction of movement of the TM1-TM2 helices. (2) Voltage-dependent MscS closed-open transitions under HHP below 50 MPa. HHP causes phospholipids to become more densely packed in the membrane bilayer. Due to lateral compressibility of the lipid bilayer, the thickness of the bilayer increases. These changes make MscS gating more difficult and less sensitive to voltage. In presence of TMAO both MscS and MscK are fully capable to gate, because channels are “shielded” with TMAO. (3) Upon further increase of HHP (50 MPa and higher) MscS and MscK the protective effect of TMAO is diminishing. At 80 MPa channels are driven to closed state regardless whether TMAO is present or not.

of TMAO the entire cytoplasmic domain should be less affected by HHP because TMAO could stabilize its structure by coordinating water around protein backbones.<sup>6</sup> As a stabilizing osmolyte TMAO is preferentially excluded from the protein surface because water is more likely than TMAO to interact favorably with the polar groups on the protein surface.<sup>7</sup> Consequently, when MscS/MscK undergoes closed-open transition, the cytoplasmic chamber stabilized by TMAO, would allow transmembrane helices to move during these transitions at HHP similar to their movement at atmospheric pressure. Given that TMAO provides primarily protection for soluble proteins it must be noted that the cytoplasmic part of MscS is exposed to water to a much greater extent than the pore forming TM3 helices. As a result the protective effect of TMAO on MscS is thus most likely due to its protective effect on the MscS cytoplasmic domain (Fig. 5B). Due to absence of MscK protein crystal structure, which can only be

deduced from the available MscS gating model, it is difficult to know how its helices may be moving during gating although it is not unreasonable to assume that they would move in a manner similar to MscS. This assumption is supported by the sequence similarity between MscS and MscK transmembrane portions and conservations of Arg residues (Arg<sup>861</sup>, Arg<sup>874</sup> and Arg<sup>878</sup>) that may serve as voltage sensors.<sup>24,57</sup>

The low free volume change of  $-13.4 \text{ \AA}^3$  in the presence of TMAO compared with the free volume change of  $-114 \text{ \AA}^3$  calculated in its absence (Fig. 4) at pressures 0–40 MPa supports findings of a number of independent studies<sup>27,32,59-61</sup> indicating a high importance of the cytoplasmic domain for the gating transitions exhibited by MscS. At pressures in the range of 40–80 MPa the free volume decrease of  $-216 \text{ \AA}^3$  is higher than the free volume change calculated in the absence of TMAO, which means that above 40 MPa, MscS/MscK were more susceptible to

HHP despite the presence of 100 mM of TMAO. Interestingly, upon the application of HHP at 80 MPa only 65% of spheroplast patches showed full recovery of the channel activity when atmospheric pressure was restored. It is possible that at pressures > 80 MPa phase transition of phospholipid membrane might occur,<sup>50</sup> which could irreversibly affect the MscS/MscK-lipid interaction thus preventing the restoration of the channel function upon release of HHP. Another possibility is that both channels may inactivate<sup>52</sup> irreversibly upon application of HHP.

A previous study investigating the effects of HHP on MscS activity suggested that the effects could mainly be due to the effects of HHP on properties of the MscS channel-associated lipid bilayer.<sup>28</sup> However, in light of the recent results reporting that a change in bilayer thickness and hydrophobic mismatch had no effect on the MscS gating,<sup>62</sup> the thickening of the bilayer caused by the increase in HHP is less likely to explain the effects of HHP reported here. Hence, given that the cytoplasmic domain of MscS is essential for its function, we believe that the results of this study indicate that HHP should predominantly act by affecting the backbone structure of the cytoplasmic domain of the MscS/MscK channel.

## Materials and Methods

**Chemicals.** All chemicals were purchased from Sigma Chemical Co.

**Bacterial strains and preparation of giant spheroplasts.** As previously described,<sup>14,36</sup> *E. coli* MscL knockout strain AW737KO was grown at 37°C in Luria-Bertani medium (10 g/l Bacto-tryptone, 5 g/l yeast extract, 5 g/l NaCl) to mid log phase (0.4–0.5 OD<sub>595</sub>). Three ml was then transferred to 27 ml fresh medium with 60 µg/ml cephalixin and cultured at 42°C on an orbital mixer incubator (Ratek) at 180 rpm until cells grew into 100–150 µm long filaments taking approx. 2–3 h. The filaments were pelleted and resuspended in 0.8 M sucrose and converted into giant spheroplasts by the addition of 50 mM Tris (pH 7.2), 200 µg/ml lysozyme and 6 mM EDTA final concentration. After addition of EDTA, the conversion process was stopped after ca. 5 min by addition of 5 mM MgCl<sub>2</sub>. The mixture of giant spheroplasts and cell debris was layered over 7-ml dilution solution containing 0.8 M sucrose, 10 mM Tris (pH 7.2), and 10 mM MgCl<sub>2</sub> in two 15 ml Falcon™ tubes and centrifuged at 1000xg for 2 min. After centrifugation the 300 µl bottom portion containing giant spheroplasts, left after removal of the supernatant with a Pasteur pipette, was diluted in 1 ml dilution solution, divided into 50 µl aliquots and stored at -20°C.

**Patch clamp and HHP setup.** An Axopatch 1D patch-clamp amplifier (Axon Corp.) combined with a home-made HHP setup was used for recording. HHP setup consisted of an oil pump, manometer, HHP chamber, oil reservoir, and a “flying-patch” device, as detailed previously.<sup>37</sup> Each experiment consisted of the following steps: (1) forming an inside-out excised patch from a spheroplast membrane, (2) testing the mechano- and voltage-sensitivity of MscS/MscK, (3) transferring the “flying-patch” device from the patch-clamp setup into the HHP chamber, (4) applying depolarizing (negative

pipette) voltage to a spheroplast patch until channels activity was observed and (5) recording the ionic current under HHP. Each HHP increase from previous to the next level has been done slowly within 10–15 sec in order to minimize heating of the preparation. Patch pipettes were pulled from borosilicate glass capillaries (Drummond Scientific Company) on a P87 pipette puller (Sutter Instruments) and had a resistance of 3–5 MΩ. Pipette solution contained 200 mM KCl, 90 mM MgCl<sub>2</sub>, 10 mM CaCl<sub>2</sub>, and 20 mM Tris, pH 7.2. Bath solution contained 200 mM KCl, 90 mM MgCl<sub>2</sub>, 10 mM CaCl<sub>2</sub>, 20 mM Tris, and 200 mM sucrose with or without 50 or 100 mM TMAO (final osmolarities) added (pH 7.2 adjusted with KOH). Gigaohm seals were formed on spheroplasts floating in the bath solution by applying gentle suction to the pipette. Inside-out excised patch recording configuration was achieved by air exposure of the patch pipette with a spheroplast on its tip. Presence of the channels in a patch was tested by applying suction and negative voltage (-30 mV) to the patch pipette. To estimate a threshold for MscS/MscK, opening steps of negative pressure were applied to the patch pipette and converted to voltage by a piezoelectric pressure transducer (Omega Engineering) with monitoring by an oscilloscope (TDS 210, Tektronix Inc.). Acquisition and data analysis software used was pClamp 9.2 (Axon Corp.) and Origin 6.1 (OriginLab).

NPo was calculated using two different methods: (1) by dividing the total current integrated over the time of recording  $\Delta t$  by the single channel current integrated over the same time  $\Delta t$ , which gives NPo as the open probability of unknown number of channels in a patch, or (2) by using the built-in utility in Clampfit 9.2 software: for each continuous recording separate NPo values were calculated for time periods when the steady-state voltage step was applied at a given HHP level. Since NPo at 0.1 MPa (1 atm) varied from patch to patch, all NPo values were normalized to the maximal value obtained during each recording. Statistical data analysis was done using Student t-test. Voltage was applied to each single patch by applying negative pipette voltage in 10 mV steps, starting from -10 mV. Patches with a voltage threshold of -80 mV or greater were excluded because of a risk of losing a gigaohm seal during application of HHP.

**Tethered bilayer setup.** The tethered bilayer<sup>38</sup> was formed by adding 8 µl of 3 mM ethanolic mobile lipid solution, to a polymer bounded 2 mm<sup>2</sup> area of tethered lipids bound to a gold surface within each well of the six well test chamber used for the experiments. The bilayer formation occurred when 100 µl of buffer was flushed through the test chamber. The incorporation of MscS or MscL was achieved by flushing with a 10 µM DDM dispersion of the corresponding MS protein in PBS buffer. This approach permits both the use of 10% tether densities and the transfer of the insoluble MS proteins into the tethered bilayer. Previous approaches have required that protein is fused with the tethered membrane by fusing proteoliposomes onto the inner leaflet tethers. Tether densities as low as 10% did not permit the latter approach as they failed to present a sufficiently hydrophobic surface to stimulate fusion. MscS and MscL proteins were prepared as previously described.<sup>39</sup>



## Conclusions

Presence of TMAO does not affect MscS/MscK voltage-sensitive gating transitions (Fig. 5.1B and 5.2B). Increasing HHP causes the bilayer thickness to increase and makes phospholipids more tightly packed. As a protective osmolyte TMAO is excluded around the surface of the cytoplasmic domain.<sup>7</sup> However, TMAO is expected to stabilize the cytoplasmic domain of MscS/MscK and protects it from the effect of HHP by coordinating water molecules around it<sup>6</sup> (shown schematically in Figure 5 as a number of TMAO molecules arranged around the cytoplasmic domain). Gating of MscS/MscK by voltage at HHP up to 40 MPa is comparable to its gating at atmospheric pressure as shown in Figure 4B. Further increase of HHP abolishes TMAO

protection of the MscS and MscK cytoplasmic domains (shown schematically in Figure 5 as reduced number of TMAO molecules coordinating water around the cytoplasmic domain). Phospholipids are more tightly packed such that the TM1-TM2 “hairpin” cannot easily move across the membrane bilayer when voltage is applied and the channel remains closed.

## Disclosure of Potential Conflicts of Interest

No potential conflicts of interest were disclosed.

## Acknowledgments

We thank Dr Oliver Friedrich for critical reading of the manuscript and suggestions for its improvement. We also gratefully acknowledge the support by the Australian Research Council.

## References

1. Mozhaev VV, Heremans K, Frank J, Masson P, Balny C. High pressure effects on protein structure and function. *Proteins* 1996; 24:81-91; PMID:8628735; [http://dx.doi.org/10.1002/\(SICI\)1097-0134\(199601\)24:1<81::AID-PROT6>3.0.CO;2-R](http://dx.doi.org/10.1002/(SICI)1097-0134(199601)24:1<81::AID-PROT6>3.0.CO;2-R).
2. Yancey PH. Organic osmolytes as compatible, metabolic and counteracting cytoprotectants in high osmolarity and other stresses. *J Exp Biol* 2005; 208:2819-30; PMID:16043587; <http://dx.doi.org/10.1242/jeb.01730>.
3. Zerbst-Boroffka I, Kamalynow RM, Harjes S, Kinne-Saffran E, Gross J. TMAO and other organic osmolytes in the muscles of amphipods (Crustacea) from shallow and deep water of Lake Baikal. *Comp Biochem Physiol A Mol Integr Physiol* 2005; 142:58-64; PMID:16139539; <http://dx.doi.org/10.1016/j.cbpa.2005.07.008>.
4. Martin DD, Bartlett, DH, Roberts MF. Solute accumulation in the deep-sea bacterium *Photobacterium profundum*. *Extremophiles* 2002; 6:507-514.
5. Molina-Höppner A, Doster W, Vogel RF, Gänzle MG. Protective effect of sucrose and sodium chloride for *Lactococcus lactis* during sublethal and lethal high-pressure treatments. *Appl Environ Microbiol* 2004; 70:2013-20; PMID:15066791; <http://dx.doi.org/10.1128/AEM.70.4.2013-2020.2004>.
6. Zou Q, Bennion BJ, Daggett V, Murphy KP. The molecular mechanism of stabilization of proteins by TMAO and its ability to counteract the effects of urea. *J Am Chem Soc* 2002; 124:1192-202; PMID:11841287; <http://dx.doi.org/10.1021/ja004206b>.
7. Street TO, Bolen DW, Rose GD. A molecular mechanism for osmolyte-induced protein stability. *Proc Natl Acad Sci U S A* 2006; 103:13997-4002; PMID:16968772; <http://dx.doi.org/10.1073/pnas.0606236103>.
8. Scarlata SF. Compression of lipid membranes as observed at varying membrane positions. *Biophys J* 1991; 60:334-40; PMID:1912276; [http://dx.doi.org/10.1016/S0006-3495\(91\)82058-6](http://dx.doi.org/10.1016/S0006-3495(91)82058-6).
9. Balny C, Masson P, Heremans K. High pressure effects on biological macromolecules: from structural changes to alteration of cellular processes. *Biochim Biophys Acta* 2002; 1595:3-10; PMID:11983383; [http://dx.doi.org/10.1016/S0167-4838\(01\)00331-4](http://dx.doi.org/10.1016/S0167-4838(01)00331-4).
10. Kato, M., Hayashi, R., Tsuda, T., and Taniguchi, K. High pressure-induced changes of biological membrane. Study on the membrane-bound Na<sup>+</sup>/K<sup>+</sup>-ATPase as a model system. *Eur J Biochem* 2002; 269:110-118.
11. Friedrich O, Kress KR, Hartmann M, Frey B, Sommer K, Ludwig H, et al. Prolonged high-pressure treatments in mammalian skeletal muscle result in loss of functional sodium channels and altered calcium channel kinetics. *Cell Biochem Biophys* 2006; 45:71-83; PMID:16679565; <http://dx.doi.org/10.1385/CBB:45:1:71>.
12. Berrier C, Besnard M, Ajouz B, Coulombe A, Ghazi A. Multiple mechanosensitive ion channels from *Escherichia coli*, activated at different thresholds of applied pressure. *J Membr Biol* 1996; 151:175-87; PMID:8661505; <http://dx.doi.org/10.1007/s002329900068>.
13. Martinac B. Mechanosensitive ion channels: molecules of mechanotransduction. *J Cell Sci* 2004; 117:2449-60; PMID:15159450; <http://dx.doi.org/10.1242/jcs.01232>.
14. Martinac B, Buechner M, Delcour AH, Adler J, Kung C. Pressure-sensitive ion channel in *Escherichia coli*. *Proc Natl Acad Sci U S A* 1987; 84:2297-301; PMID:2436228; <http://dx.doi.org/10.1073/pnas.84.8.2297>.
15. Sukharev SI, Martinac B, Arshavsky VY, Kung C. Two types of mechanosensitive channels in the *Escherichia coli* cell envelope: solubilization and functional reconstitution. *Biophys J* 1993; 65:177-83; PMID:7690260; [http://dx.doi.org/10.1016/S0006-3495\(93\)81044-0](http://dx.doi.org/10.1016/S0006-3495(93)81044-0).
16. Berrier C, Coulombe A, Houssin C, Ghazi A. A patch-clamp study of ion channels of inner and outer membranes and of contact zones of *E. coli*, fused into giant liposomes. Pressure-activated channels are localized in the inner membrane. *FEBS Lett* 1989; 259:27-32; PMID:2480919; [http://dx.doi.org/10.1016/0014-5793\(89\)81486-3](http://dx.doi.org/10.1016/0014-5793(89)81486-3).
17. Delcour AH, Martinac B, Adler J, Kung C. Modified reconstitution method used in patch-clamp studies of *Escherichia coli* ion channels. *Biophys J* 1989; 56:631-6; PMID:2477074; [http://dx.doi.org/10.1016/S0006-3495\(89\)82710-9](http://dx.doi.org/10.1016/S0006-3495(89)82710-9).
18. Vásquez V, Cortes DM, Furukawa H, Perozo E. An optimized purification and reconstitution method for the MscS channel: strategies for spectroscopic analysis. *Biochemistry* 2007; 46:6766-73; PMID:17500538; <http://dx.doi.org/10.1021/bi700322k>.
19. Martinac B, Adler J, Kung C. Mechanosensitive ion channels of *E. coli* activated by amphipaths. *Nature* 1990; 348:261-3; PMID:1700306; <http://dx.doi.org/10.1038/348261a0>.
20. Martinac, B. Mechanosensitive channels in prokaryotes. *Cell Physiol Biochem* 2011; 11:61-76.
21. Sukharev S. Purification of the small mechanosensitive channel of *Escherichia coli* (MscS): the subunit structure, conduction, and gating characteristics in liposomes. *Biophys J* 2002; 83:290-8; PMID:12080120; [http://dx.doi.org/10.1016/S0006-3495\(02\)75169-2](http://dx.doi.org/10.1016/S0006-3495(02)75169-2).
22. Bass RB, Strop P, Barclay M, Rees DC. Crystal structure of *Escherichia coli* MscS, a voltage-modulated and mechanosensitive channel. *Science* 2002; 298:1582-7; PMID:12446901; <http://dx.doi.org/10.1126/science.1077945>.
23. Steinbacher S, Bass R, Strop P, Rees DC. (2007). Structures of the prokaryotic mechanosensitive channels MscL and MscS. In *Mechanosensitive Ion Channels, Part A, Volume 58*. (San Diego: Elsevier Academic Press Inc), pp. 1-24.
24. Bezanilla F, Perozo E. Structural biology. Force and voltage sensors in one structure. *Science* 2002; 298:1562-3; PMID:12446894; <http://dx.doi.org/10.1126/science.1079369>.
25. Miller S, Edwards MD, Ozdemir C, Booth IR. The closed structure of the MscS mechanosensitive channel. Cross-linking of single cysteine mutants. *J Biol Chem* 2003; 278:32246-50; PMID:12767977; <http://dx.doi.org/10.1074/jbc.M303188200>.
26. Markin VS, Martinac B. Mechanosensitive ion channels as reporters of bilayer expansion. A theoretical model. *Biophys J* 1991; 60:1120-7; PMID:1723115; [http://dx.doi.org/10.1016/S0006-3495\(91\)82147-6](http://dx.doi.org/10.1016/S0006-3495(91)82147-6).
27. Sotomayor M, van der Straaten TA, Ravaoli U, Schulten K. Electrostatic properties of the mechanosensitive channel of small conductance MscS. *Biophys J* 2006; 90:3496-510; PMID:16513774; <http://dx.doi.org/10.1529/biophysj.105.080069>.
28. Macdonald AG, Martinac B. Effect of high hydrostatic pressure on the bacterial mechanosensitive channel MscS. *Eur Biophys J* 2005; 34:434-41; PMID:15834558; <http://dx.doi.org/10.1007/s00249-005-0478-8>.
29. Hurst AC, Petrov E, Kloda A, Nguyen T, Hool L, Martinac B. MscS, the bacterial mechanosensitive channel of small conductance. *Int J Biochem Cell Biol* 2008; 40:581-5; PMID:17466568; <http://dx.doi.org/10.1016/j.biocel.2007.03.013>.
30. Koprowski P, Kubalski A. Voltage-independent adaptation of mechanosensitive channels in *Escherichia coli* protoplasts. *J Membr Biol* 1998; 164:253-62; PMID:9691118; <http://dx.doi.org/10.1007/s002329900410>.
31. Perozo E. Gating prokaryotic mechanosensitive channels. *Nat Rev Mol Cell Biol* 2006; 7:109-19; PMID:16493417; <http://dx.doi.org/10.1038/nrm1833>.
32. Sotomayor M, Schulten K. Molecular dynamics study of gating in the mechanosensitive channel of small conductance MscS. *Biophys J* 2004; 87:3050-65; PMID:15339798; <http://dx.doi.org/10.1529/biophysj.104.046045>.
33. Rowe I, Kamaraju K, Boer M, Belyy V, Anishkin A, Sukharev S. The Hollow Domain of the Mechanosensitive Channel MscS is a Sensor of Cytoplasmic Crowding. *Biophys J* 2012; 102:121a; <http://dx.doi.org/10.1016/j.bpj.2011.11.679>.
34. Levina N, Töttemeyer S, Stokes NR, Louis P, Jones MA, Booth IR. Protection of *Escherichia coli* cells against extreme turgor by activation of MscS and MscL mechanosensitive channels: identification of genes required for MscS activity. *EMBO J* 1999; 18:1730-7; PMID:10202137; <http://dx.doi.org/10.1093/emboj/18.7.1730>.
35. Perozo E, Rees DC. Structure and mechanism in prokaryotic mechanosensitive channels. *Curr Opin Struct Biol* 2003; 13:432-42; PMID:12948773; [http://dx.doi.org/10.1016/S0959-440X\(03\)00106-4](http://dx.doi.org/10.1016/S0959-440X(03)00106-4).

36. Ruthe HJ, Adler J. Fusion of bacterial spheroplasts by electric fields. *Biochim Biophys Acta* 1985; 819:105-13; PMID:3899175; [http://dx.doi.org/10.1016/0005-2736\(85\)90200-7](http://dx.doi.org/10.1016/0005-2736(85)90200-7).
37. Macdonald AG, Martinac B. Effect of high hydrostatic pressure on the porin OmpC from *Escherichia coli*. *FEMS Microbiol Lett* 1999; 173:327-34; PMID:10227163; <http://dx.doi.org/10.1111/j.1574-6968.1999.tb13521.x>.
38. Cornell BA, Braach-Maksvytis VL, King LG, Osman PD, Raguse B, Wiczorek L, et al. A biosensor that uses ion-channel switches. *Nature* 1997; 387:580-3; PMID:9177344; <http://dx.doi.org/10.1038/42432>.
39. Martinac B, Rohde PR, Battle AR, Petrov E, Pal P, Foo AF, et al. Studying mechanosensitive ion channels using liposomes. *Methods Mol Biol* 2010; 606:31-53; PMID:20013388; [http://dx.doi.org/10.1007/978-1-60761-447-0\\_4](http://dx.doi.org/10.1007/978-1-60761-447-0_4).
40. Kung C, Martinac B, Sukharev S. Mechanosensitive channels in microbes. *Annu Rev Microbiol* 2010; 64:313-29; PMID:20825352; <http://dx.doi.org/10.1146/annurev.micro.112408.134106>.
41. Martinac B, Saimi Y, Kung C. Ion channels in microbes. *Physiol Rev* 2008; 88:1449-90; PMID:18923187; <http://dx.doi.org/10.1152/physrev.00005.2008>.
42. Edwards MD, Li Y, Kim S, Miller S, Bartlett W, Black S, et al. Pivotal role of the glycine-rich TM3 helix in gating the MscS mechanosensitive channel. *Nat Struct Mol Biol* 2005; 12:113-9; PMID:15665866; <http://dx.doi.org/10.1038/nsmb895>.
43. Hamill OP, Martinac B. Molecular basis of mechanotransduction in living cells. *Physiol Rev* 2001; 81:685-740; PMID:11274342.
44. Perozo E, Cortes DM, Sompormpisut P, Kloda A, Martinac B. Open channel structure of MscL and the gating mechanism of mechanosensitive channels. *Nature* 2002; 418:942-8; PMID:12198539; <http://dx.doi.org/10.1038/nature00992>.
45. Corry B. An energy-efficient gating mechanism in the acetylcholine receptor channel suggested by molecular and Brownian dynamics. *Biophys J* 2006; 90:799-810; PMID:16284265; <http://dx.doi.org/10.1529/biophysj.105.067868>.
46. Vora T, Corry B, Chung SH. Brownian dynamics investigation into the conductance state of the MscS channel crystal structure. *Biochim Biophys Acta* 2006; 1758:730-7; PMID:16781663; <http://dx.doi.org/10.1016/j.bbame.2006.04.014>.
47. Sachs F. Mechanical transduction in biological systems. *Crit Rev Biomed Eng* 1988; 16:141-69; PMID:2460290.
48. Sachs F. Stretch-activated ion channels: what are they? *Physiology* (Bethesda) 2010; 25:50-6; PMID:20134028; <http://dx.doi.org/10.1152/physiol.00042.2009>.
49. Martinac B. Bacterial mechanosensitive channels as a paradigm for mechanosensory transduction. *Cell Physiol Biochem* 2011; 28:1051-1060.
50. Perrier-Cornet JM, Baddouj K, Gervais P. Pressure-induced shape change of phospholipid vesicles: implication of compression and phase transition. *J Membr Biol* 2005; 204:101-7; PMID:16245032; <http://dx.doi.org/10.1007/s00232-005-0752-9>.
51. Sotomayor M, Vásquez V, Perozo E, Schulten K. Ion conduction through MscS as determined by electrophysiology and simulation. *Biophys J* 2007; 92:886-902; PMID:17114233; <http://dx.doi.org/10.1529/biophysj.106.095232>.
52. Akitake B, Anishkin A, Sukharev S. The "dashpot" mechanism of stretch-dependent gating in MscS. *J Gen Physiol* 2005; 125:143-54; PMID:15657299; <http://dx.doi.org/10.1085/jgp.200409198>.
53. Beney L, Perrier-Cornet JM, Hayert M, Gervais P. Shape modification of phospholipid vesicles induced by high pressure: influence of bilayer compressibility. *Biophys J* 1997; 72:1258-63; PMID:9138571; [http://dx.doi.org/10.1016/S0006-3495\(97\)78772-1](http://dx.doi.org/10.1016/S0006-3495(97)78772-1).
54. Braganza LF, Worcester DL. Structural changes in lipid bilayers and biological membranes caused hydrostatic pressure. *Biochemistry* 1986; 25:7484-8; PMID:3801427; <http://dx.doi.org/10.1021/bi00371a034>.
55. Perozo E, Kloda A, Cortes DM, Martinac B. Physical principles underlying the transduction of bilayer deformation forces during mechanosensitive channel gating. *Nat Struct Biol* 2002; 9:696-703; PMID:12172537; <http://dx.doi.org/10.1038/nsb827>.
56. Martinac B, Hamill OP, Gramicidin A channels switch between stretch activation and stretch inactivation depending on bilayer thickness. *Proc Natl Acad Sci U S A* 2002; 99:4308-12; PMID:11904391; <http://dx.doi.org/10.1073/pnas.072632899>.
57. Bass RB, Strop P, Barclay M, Rees DC. Crystal structure of *Escherichia coli* MscS, a voltage-modulated and mechanosensitive channel. *Science* 2002; 298:1582-7; PMID:12446901; <http://dx.doi.org/10.1126/science.1077945>.
58. Edwards MD, Booth IR, Miller S. Gating the bacterial mechanosensitive channels: MscS a new paradigm? *Curr Opin Microbiol* 2004; 7:163-7; PMID:15063854; <http://dx.doi.org/10.1016/j.mib.2004.02.006>.
59. Miller S, Bartlett W, Chandrasekaran S, Simpson S, Edwards M, Booth IR. Domain organization of the MscS mechanosensitive channel of *Escherichia coli*. *EMBO J* 2003; 22:36-46; PMID:12505982; <http://dx.doi.org/10.1093/emboj/cdg011>.
60. Grajkowski W, Kubalski A, Koprowski P. Surface changes of the mechanosensitive channel MscS upon its activation, inactivation, and closing. *Biophys J* 2005; 88:3050-9; PMID:15665126; <http://dx.doi.org/10.1529/biophysj.104.053546>.
61. Schumann U, Edwards MD, Li C, Booth IR. The conserved carboxy-terminus of the MscS mechanosensitive channel is not essential but increases stability and activity. *FEBS Lett* 2004; 572:233-7; PMID:15304354; <http://dx.doi.org/10.1016/j.febslet.2004.07.045>.
62. Nomura T, Cranfield CG, Deplazes E, Owen DM, Macmillan A, Battle AR, et al. Differential effects of lipids and lyso-lipids on the mechanosensitivity of the mechanosensitive channels MscL and MscS. *Proc Natl Acad Sci U S A* 2012; 109:8770-5; PMID:22586095; <http://dx.doi.org/10.1073/pnas.12000511109>.